JACS
JOURNAL OF THE AMERICAN CHEMICAL SOCIETY
pubs.acs.org/JACS
Article

Catalytic 1,3-Proton Transfer in Alkenes Enabled by Fe=NR Bond Cooperativity: A Strategy for pK_a-Dictated Regioselective Transposition of C=C Double Bonds

Yafei Gao, Xuelian Li, Jeremiah E. Stevens, Hao Tang,* and Jeremy M. Smith*

Cite This: *J. Am. Chem. Soc.* 2023, 145, 11978–11987
Read Online
ACCESS | Metrics & More | Article Recommendations | Supporting Information

ABSTRACT: Transition metal catalyzed alkene double bond transposition usually involves metal hydride intermediates. Despite significant advances in the design of catalysts that dictate product selectivity, control over substrate selectivity is less advanced and transition metal catalysts that selectively transpose double bonds in substrates containing multiple 1-alkene functionalities are rare. Herein, we report that the three-coordinate high spin (S = 2) Fe(II) imido complex [$Ph_2B(^tBuIm)_2Fe$=NDipp][K(18-C-6)THF_2] (**1-K(18-C-6)**) catalyzes 1,3-proton transfer from 1-alkene substrates to afford 2-alkene transposition products. Mechanistic investigations involving kinetics, competition, and isotope labeling studies, supported by experimentally calibrated DFT computations, strongly support an unusual nonhydridic mechanism for alkene transposition that is enabled by the cooperative action of the iron center and basic imido ligand. As dictated by the pK_a of the allylic protons, this catalyst enables the regioselective transposition of C=C double bonds in substrates containing multiple 1-alkenes. The high spin (S = 2) state of the complex allows a wide scope of functional groups to be tolerated, including those that are typical catalyst poisons, such as amines, *N*-heterocycles, and phosphines. These results demonstrate a new strategy for metal-catalyzed alkene transposition with predictable substrate regioselectivity.

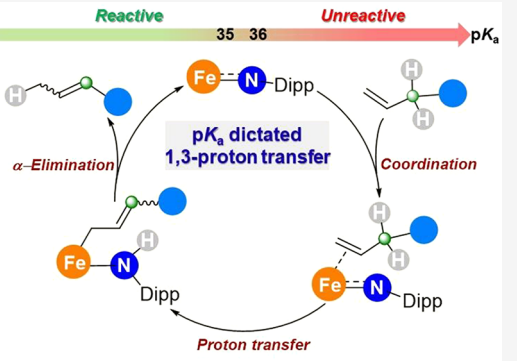

INTRODUCTION

The transition metal catalyzed positional transposition of alkenes is an atom-economical transformation with many applications in natural and industrial products synthesis.[1−4] The importance of this transformation is illustrated in part through the numerous reports over the past decade for highly efficient noble (e.g., Ru, Rh, Pd and Ir) and base metal (e.g., Fe, Co and Ni) catalysts that facilitate the transposition of terminal to internal alkenes.[5−15]

Despite significant advances in this field, catalyst-controlled selectivity in alkene transposition is still a challenge. Generally, three kinds of selectivity can be considered, two of which are concerned with product selectivity (Scheme 1A). First, for substrates where there may be multiple energetically similar products resulting from double bond transposition, catalysts can dictate positional selectivity by controlling the extent of double bond transposition via the "chain walking" process.[16] While changing positional selectivity often requires a change in catalyst,[11] a recent report has elegantly demonstrated this can be achieved using a Na^+-responsive iridium catalyst (Scheme 1A, a).[17] Second, the geometrical selectivity of the transposed alkene, as determined by the E/Z ratio, can also be controlled by the catalyst, often by hindering formation of the thermodynamically favored E isomer (Scheme 1A, b).[7] A leading strategy is the use of bulky metal catalysts, e.g., cobalt β-diketiminates, that sterically favor the Z isomer.[18] Finally, regioselective alkene transposition requires the selective movement of one double bond in substrates containing multiple alkene functionalities. This transformation is important for the synthesis of complex molecules. For example, the regioselective transposition of an alkene at one position over others in the same molecule may be required to construct specific ring sizes by subsequent ring-closing metathesis reactions.[19]

The challenges toward controlling substrate regioselectivity can be understood in the context of the known mechanisms for transition metal catalyzed alkene transposition. Four mechanisms are generally proposed, namely the alkyl, π-allyl, hydrogen atom transfer (HAT), and metalloradical induced H atom relocation mechanisms (Scheme 1B, a−d).[10,18,20−24] Despite their differences, it is notable that they all involve transition metal hydride intermediates that are predisposed to react with sterically accessible 1-alkenes. In the case of catalysts

Received: December 14, 2022
Published: May 25, 2023

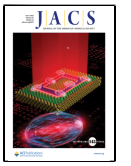

https://doi.org/10.1021/jacs.2c13350
J. Am. Chem. Soc. 2023, 145, 11978−11987

Scheme 1. Transition Metal Catalyzed Alkene Transposition

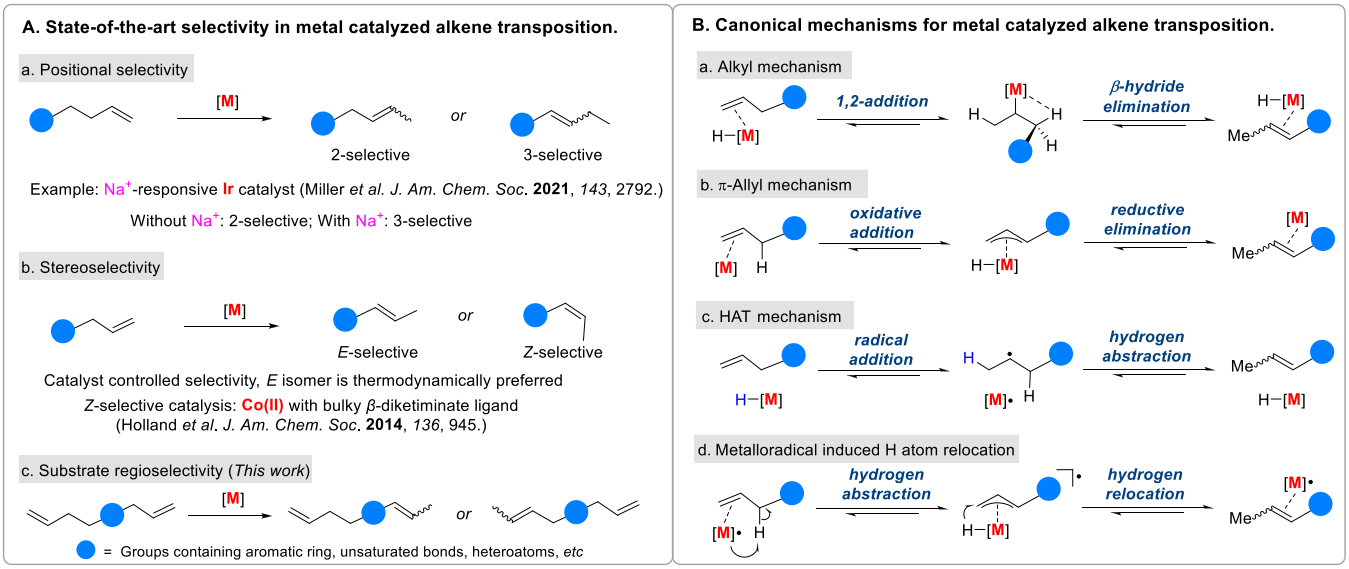

that follow the HAT mechanism, transposition is fastest for the alkenes that best stabilize radicals, which often favors the more highly substituted product.[21] Nonetheless, controlling substrate selectivity in substrates having multiple 1-alkenes is still a challenge (Scheme 1A, c).[5−7]

We hypothesized that a mechanism involving the base-facilitated motion of a proton from an allylic C−H bond would provide a strategy for the regioselective alkene transposition. Here, the pK_a of the allylic C−H bond is expected to provide a means for controlling the substrate regioselectivity. Indeed, it has been known for some time that strong bases (e.g., ^{t}BuO$^-$ in DMSO) are able to mediate the transposition of double bonds in phenylpropenoids.[25,26]

The extensive work on metal−ligand cooperativity in catalytic reactions involving proton transfer provides an intellectual framework for the design of alkene transposition catalysts.[27] For example, the cooperative action of metal and ligand in proton transfer enables transformations that include the catalytic carboetherification of allenol,[28] the dimerization of terminal alkynes,[29] and the hydroamination of alkynes.[30] It is notable that these reactions involve proton transfer from relatively acidic −OH, C(sp)−H, and −NH$_2$ protons (pK_a < 30 in DMSO) to weakly basic ketone and pyridine moieties of the ligand. Building on these precedents, we envisioned that the cooperative action of a transition metal center and a highly basic ligand would allow for similar proton transfer of weakly acidic protons, such as those in the allylic position (pK_a > 30 in DMSO). Alkene transposition would then be initiated by intramolecular proton transfer from a coordinated alkene. It is worth mentioning that Grotjahn had proposed such metal−ligand cooperativity in the mechanism of a CpRu(PN) catalyzed alkene transposition reaction,[31,32] although this idea was not borne out in a subsequent comprehensive experimental and computational investigation. Instead, transposition was found to occur by the π-allyl mechanism.[33]

In principle, the high basicity of dianionic imido (NR^{2-}) ligands makes them well-suited to removing suitably acidic allylic protons from alkenes. However, this is not characteristic of their reactivity, and metal imido complexes generally react with alkenes in [2 + 2] cycloadditions, nitrene transfer and C−H insertion reactions (Scheme 2A).[34−48] Nonetheless,

Scheme 2. Reaction Patterns of Transition Metal Imido Complexes with Alkenes

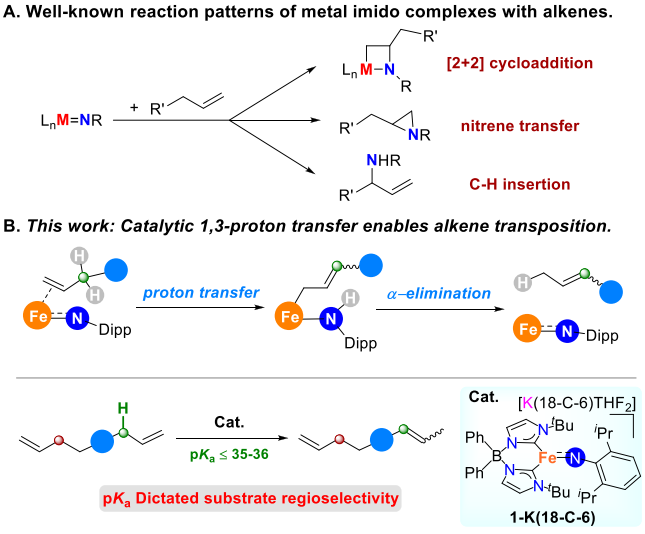

appropriate molecular design has been shown to enable alternate reaction pathways. Notably, Arnold, Toste and co-workers have reported that the "π-loaded" vanadium bis(imido) complex $[(PMe_3)_3V(N^tBu)_2]^+$ catalyzes the semi-hydrogenation of alkynes to *Z*-alkenes.[49] Here, mechanistic studies implicate the cooperative action of vanadium and the imido ligand in H_2 activation to afford new amido and hydride ligands. Subsequent alkyne insertion and 1,2-α-NH-elimination regenerate the bis(imido) catalyst. The utility of such metal-imido cooperativity in catalysis, which would potentially allow for unusual transformations, has been barely investigated.

Some of us previously reported the Fe(II) imido complex $[Ph_2B(^tBuIm)_2Fe{=}NDipp][K(18\text{-}C\text{-}6)THF_2]$ (**1-K(18-C-6)**), in which the low-valent, high-spin iron center imparts unusual basicity/nucleophilicity on the imido ligand, as modulated by the coordination of alkali ions.[50−52] The strong basicity/nucleophilicity of the imido ligand enables unusual reactions for a late metal imido ligand, including the formal insertion of carbodiimides into the Fe=NR bond. Of greater

https://doi.org/10.1021/jacs.2c13350
J. Am. Chem. Soc. 2023, 145, 11978−11987

relevance to the current manuscript are the first examples of ene-like reactions of a M=NR bond with internal alkynes and nitriles, which are for the basis of catalytic alkyne and nitrile α-deuteration reactions, respectively. In these reactions, the imido ligand acts as a proton shuttle.

Continuing our efforts in developing the basic imido ligand in catalysis, herein, we report the unusual catalytic reactivity of **1-K(18-C-6)** with alkene substrates, in which the iron center and the basic imido ligand cooperatively facilitate 1,3-proton transfer from a coordinated 1-alkene substrate to generate the corresponding 2-alkene (Scheme 2B). Experimental mechanistic studies, along with experimentally calibrated DFT calculations, show that both the metal and imido ligand are critical to catalysis. This catalyst enables double bond transposition for a variety of alkenes, as dictated by the pK_a of the allylic protons. A wide scope of functional groups that are typical catalyst poisons are tolerated by the catalyst, which we attribute to its high spin nature. This pK_a-dictated reactivity provides a new strategy for transition metal catalyzed regioselective double bond transposition in substrates containing multiple 1-alkene functionalities.

RESULTS AND DISCUSSION

Reaction Design and Mechanistic Studies. We previously demonstrated that the basic imido ligand in **1-K(18-C-6)** enables ene-like reactivity of the Fe=NR bond with internal alkynes and nitriles,[51] where proton transfer from the α-position of the alkynes and nitriles to the imido ligand affords Fe amido allenyl and Fe amido keteniminate complexes, respectively (pK_a(N≡CC**H**$_2$Me) = 32.5 in DMSO).[53] In light of this observation, we reasoned that the acidic allylic protons of alkenes may react similarly, providing an entry point to double bond transposition. Subsequent 1,2-α-CH-elimination from the resulting amido alkyl complex would regenerate **1-K(18-C-6)** along with the transposed alkenes (Scheme 2B).

Since its benzylic protons are of comparable acidity (pK_a ≈ 33 in DMSO),[54] we identified allylbenzene (**2a**) as an appropriate substrate for testing our hypothesis. Gratifyingly, in the presence of 5 mol % **1-K(18-C-6)**, **2a** undergoes proton transfer to enable formation of the double-bond transposed product prop-1-en-1-ylbenzene **2b** over the course of 6 h at room temperature (Table 1, entry 1). The product is obtained in high yield with *E*/*Z* selectivity (94:6) that is comparable to many other transition metal catalysts.[55−57] Similarly, allylbenzenes (**3a**−**9a**) bearing a range of functional groups also undergo double bond transposition to the corresponding *E*-prop-1-en-1-ylbenzenes (**3b**−**9b**) in good yields and with high *E*/*Z* ratios (entries 2−8). While transposition is observed for substrates bearing both strong donors and weakly electron withdrawing groups, no transposition is observed for very strong electron withdrawing groups (e.g., 4-CF_3). Catalytic transposition of a 1,1-disubstituted allylbenzene (**10a**) and internal allylbenzene (**11a**) are also observed (entries 9−10), although moderate heating and/or a higher catalyst loading are required for these substrates, likely due to their increased steric hindrance. It is important to note that there is no evidence for the formation of naphthalene from **11a**, suggesting that catalysis does not occur by a mechanism involving hydrogen atom transfer (HAT).

To the best of our knowledge, the catalytic transposition of alkenes by an imido complex is unprecedented.[58,59] As mentioned earlier, metal imido complexes either react with alkenes in [2 + 2] cycloaddition reactions to afford four-membered metallacycles or undergo nitrene transfer to provide aziridination or C−H amination products. In light of this unique activity, we undertook a series of investigations involving kinetics, competition studies, isotope labeling, stoichiometric reactions, and DFT calculations to shed light on the mechanism of catalysis.

Table 1. Catalytic 1,3-Proton Transfer of Allylbenzenes Using 1-K(18-C-6)[a]

Entry	Substrate	Time	*E*/*Z*	Product	Yield
1	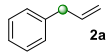 **2a**	6 h	94:6	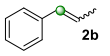 **2b**	92%
2	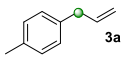 **3a**	12 h	94:6	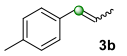 **3b**	90%
3	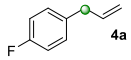 **4a**	4 h	92:8	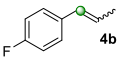 **4b**	88%
4	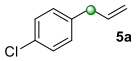 **5a**	4 h	93:7	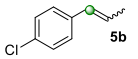 **5b**	91%
5	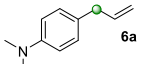 **6a**	12 h	93:7	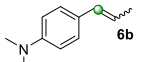 **6b**	92%[b]
6	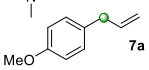 **7a**	20 h	88:12	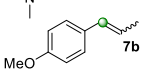 **7b**	95%
7	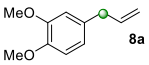 **8a**	3 h	95:5	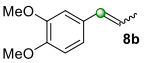 **8b**	95%
8	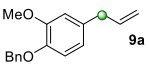 **9a**	12 h	92:8	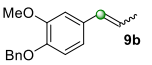 **9b**	93%
9	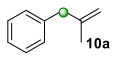 **10a**	24 h	-	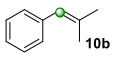 **10b**	85%[c]
10	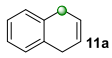 **11a**	15 h	-	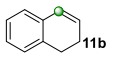 **11b**	96%[b]

[a]Reaction conditions: alkene (0.5 mmol) with 5 mol % **1-K(18-C-6)** at room temperature in 0.5 mL of THF-d_8; the yields were obtained by ^{1}H NMR analysis of the crude material using mesitylene as internal standard, and the conversions for the substrates are >99%. [b]50 °C. [c]10 mol % **1-K(18-C-6)** at 50 °C.

Involvement of Iron. We first undertook experiments to delineate the nature of catalytically active species. Since strong bases are known to catalyze double bond transposition, it is conceivable that **1-K(18-C-6)** is the source of a strong base that is the actual catalyst. While we have never observed its formation from **1-K(18-C-6)**, DippNH$^-$ is the most likely candidate for being generated under catalytic conditions. Here, we find that the rate of double bond transposition for **2a** with DippNH$^-$ is considerably slower (70% after 5 days at rt) than with **1-K(18-C-6)**, suggesting that catalysis involves the iron complex.[60]

Given the coordinatively unsaturated nature of the metal ion in **1-K(18-C-6)** (Figure S84), we hypothesized that the reaction mechanism involves initial coordination of the alkene to iron. Indeed, we have previously observed that **1-K(18-C-6)** can bind an additional ligand.[51] To test this, we investigated the transposition of allylbenzene in the presence of equimolar 1-octene (Figure S59), which does not undergo catalytic transposition by **1-K(18-C-6)** (see below). This experiment reveals that there is a 4-fold decrease in the rate of allylbenzene transposition in the presence of 1-octene (Figure S70). This suggests that there is competitive coordination of 1-octene to

https://doi.org/10.1021/jacs.2c13350
J. Am. Chem. Soc. 2023, 145, 11978−11987

the catalyst, and that the transposition mechanism requires the alkene substrate to coordinate to iron. Further support for this hypothesis comes from the observation that **1-K(18-C-6)** is a catalyst for the *cis* to *trans* isomerization of *cis*-stilbene (Figure S81). As with 1-octene, the rate allylbenzene transposition is inhibited by the presence of *cis*-stilbene (Figure S70).[61]

Involvement of the Imido Ligand. To test whether the imido ligand plays a role in catalysis, we investigated the transposition of **2a** using the alkali metal ion-coordinated imido complexes $[Ph_2B(^tBuIm)_2Fe{=}NDippK]_2$ (**1-K**), $[Ph_2B(^tBuIm)_2Fe{=}NDippNa(THF)_3]$ (**1-Na**), and $[Ph_2B(^tBuIm)_2Fe{=}NDippLi(THF)_2]$ (**1-Li**) as catalysts (Figure 1). Here, we observe that the rate of transposition is strongly

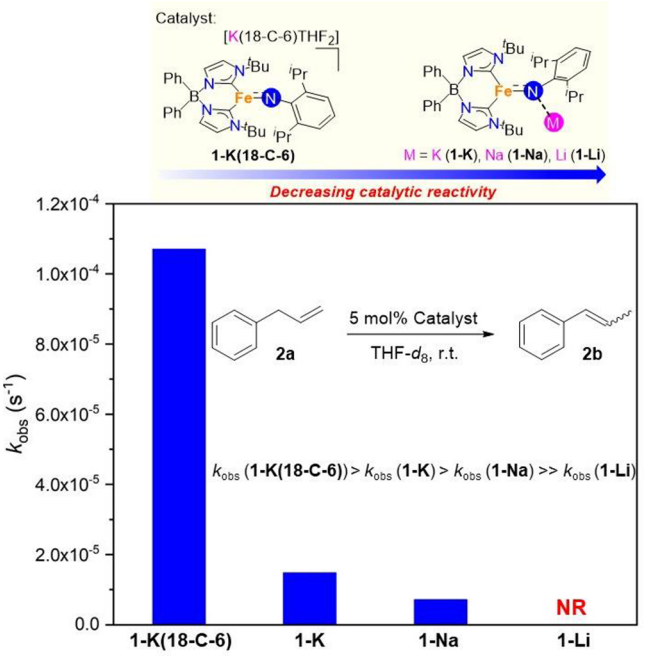

Figure 1. Rates of **2a** transposition using 5 mol % **1-K(18-C-6)** and **1-K/Na/Li** as the catalyst at room temperature in THF-d_8. For **1-K(18-C-6)**, **1-K**, **1-Na**, and **1-Li**, k_{obs} = 1.07 × 10^{-4}, 1.48 × 10^{-5}, 7.11 × 10^{-6}, and 0 s^{-1}, respectively.

dependent on the alkali metal ion, with the rate decreasing by 2 orders of magnitude according to **1-K(18-C-6)** > **1-K** > **1-Na**.[62] No transposition is observed for the lithium coordinated complex **1-Li**. We have previously demonstrated that smaller alkali metal ions bind more tightly to the imido ligand, decreasing its accessibility to external substrates.[52] The dependence of the transposition rate on the size of the alkali metal ion strongly suggests that the imido ligand plays a key role in the transposition mechanism. This is further supported by the inhibitory effect of added aniline. Specifically, at 45 °C transposition of **2a** by **1-K(18-C-6)** requires more than 3 d in the presence of 5 mol % H_2NDipp.[63] We have previously shown that bis(anilido) complex $[Ph_2B(^tBuIm)_2Fe(NHDipp)_2]^-$ is formed from **1-K(18-C-6)** and H_2NDipp.[50] This latter result also supports the involvement of iron in the alkene transposition catalysis.

Additional Mechanistic Experiments. We used deuterium labeling experiments to provide additional mechanistic insight. The basicity of the imido ligand suggests that double bond transposition involves deprotonation of the coordinated alkene substrate. To test this, we investigated the transposition of **2a-d_2**, which is selectively deuterated at the benzylic positions. We observe that transposition of substrate to **2b-d_2** (Scheme 3a) occurs at a rate that is significantly slower than

Scheme 3. Deuterium Labelling Studies

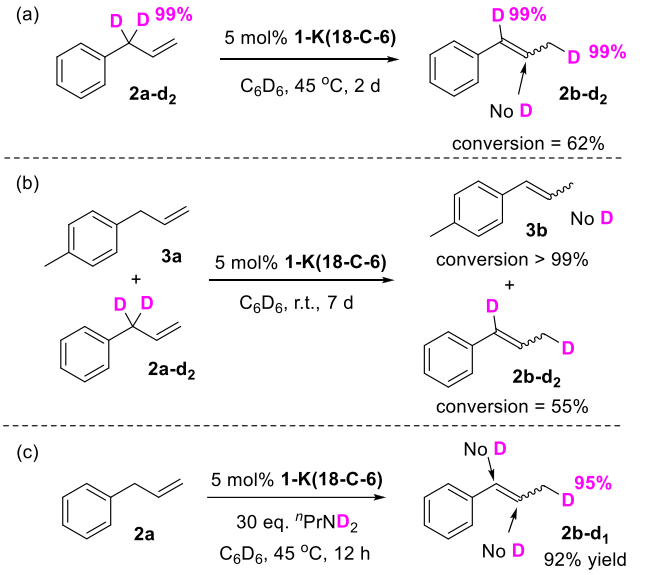

that for **2a** under the same conditions, with kinetic isotope effect (KIE), k_H/k_D = 34 at 40 °C.[64,65] Importantly, a crossover experiment involving **3a** and **2a-d_2** does not lead to any deuterium incorporation in **3b** (Scheme 3b), suggesting the proton transfer from the alkene to imido ligand is intra- and not intermolecular.

Further support for proton transfer comes from the positive slope (ρ = 1.54) in the Hammett plot for the transposition of a series of *para*-substituted allylbenzenes (Figure 2). It is important to note that the rate of catalysts is not dependent on the benzylic C−H bond BDFEs, as would be expected for a mechanism involving HAT (Figure S95).

A different isotope labeling experiment provides evidence for an amido η^1-allyl iron intermediate, akin to the previously observed formation of allenyl ligands from alkynes.[51] Trans-

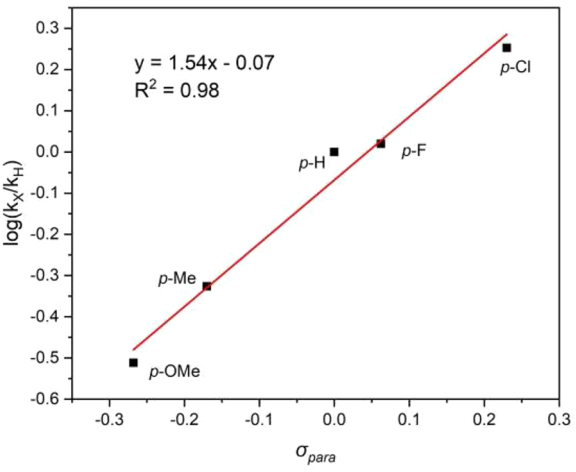

Figure 2. Linear free energy correlation of $\log(k_X/k_H)$ *vs* σ_p for the transposition of *para*-substituted allylbenzenes using **1-K(18-C-6)** as the catalyst.

https://doi.org/10.1021/jacs.2c13350
J. Am. Chem. Soc. 2023, 145, 11978−11987

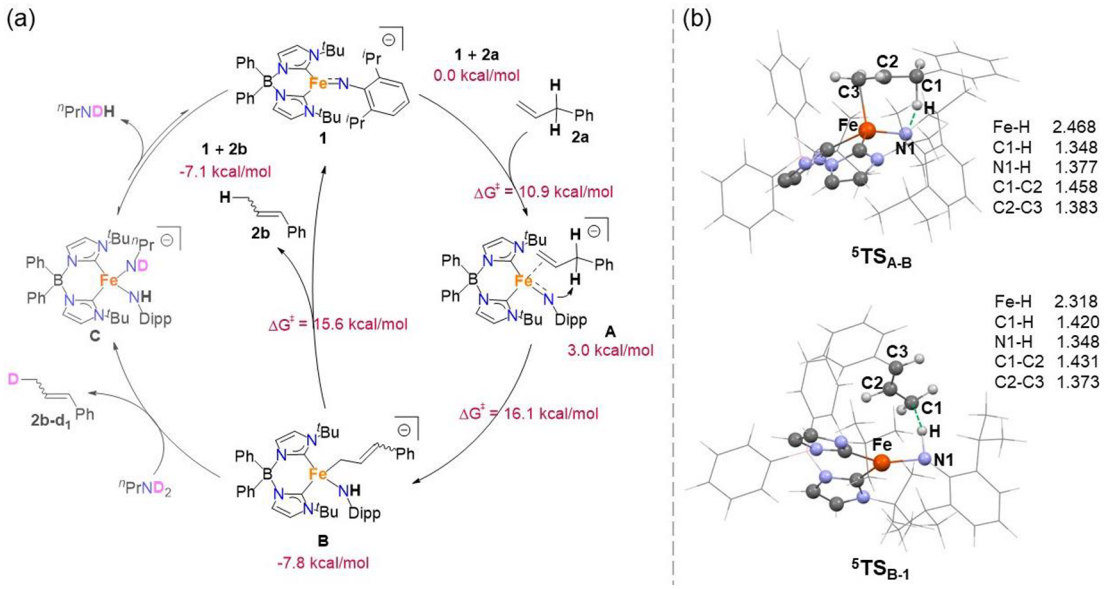

Figure 3. (a) Experimentally and computationally proposed catalytic cycle for alkene transposition of **2a** by **1-K(18-C-6)**, along with the calculated energy profile (BP86/B2/SMD//M06L/B1/GP) (all the energies are relative to **1** + **2a**). (b) Calculated transition states ^{5}**TS**$_{\mathbf{A\text{-}B}}$ and ^{5}**TS**$_{\mathbf{B\text{-}1}}$ with selected bond distances (Å).

position of **2a** in the presence of excess ^{n}PrND$_2$ affords **2b-d$_1$** (Scheme 3c), where there is exclusive monodeuteration of the methyl group of the *E*-prop-1-en-1-ylbenzene product (up to 95% deuterium incorporation). This is consistent with proton transfer from the alkene to the imido ligand to afford an η^1-allyl ligand, which is in turn protonated by ^{n}PrND$_2$ to yield **2b-d$_1$** concomitant with formation of the complex [Ph$_2$B(^{t}BuIm)$_2$Fe(NHDipp)(ND^{n}Pr)]$^-$ (Figure 3a and Figure S60).

Deuterium labeling experiments also exclude mechanisms involving simple base deprotonation. For example, with 5 mol % ^{n}PrNH$^-$ catalyst,[66] full deuteration of the methyl group (~90%) in the transposition product **2b** is observed (Figures S55−S56), in contrast to monodeuteration with **1-K(18-C-6)**. Similarly, deuterium labeling experiments with DippNH$^-$ catalyst result in <20% of **2b-d$_1$** (Figures S57−S58), along with other deuterated species, providing further evidence that DippNH$^-$ is not the active catalyst.

Characterization of a Catalytically Competent Intermediate. Stoichiometric experiments provide further support for a mechanism involving the cooperative action of iron and the imido ligand. Reaction of **1-K(18-C-6)** with equimolar allylbenzene **2a** leads to the formation of a new complex. While its instability in solution has thwarted attempts to crystallographically characterize this species, its spectroscopic properties and reactivity are consistent with the four-coordinate high-spin (*S* = 2) Fe(II) η^1-allyl amido complex **B** (Scheme 4, see also Figure 3).

In addition to ^{1}H NMR spectroscopy, complex **B** has been characterized by zero field ^{57}Fe Mössbauer spectroscopy. Here, the spectral parameters (δ = 0.76 mm/s and ΔE_Q = 2.85 mm/s, Figure S83) are consistent with those observed for tetrahedral high spin Fe(II) complexes.[51] Notably, these parameters are very similar to those observed for the previously reported Fe(II) amido allenyl complex [Ph$_2$B(^{t}BuIm)$_2$Fe(NHDipp)((Et)C═C═C(Me)(H))]$^-$ (δ = 0.70 mm/s and ΔE_Q = 3.11 mm/s),[51] suggesting a similar coordination environment at iron.

Scheme 4. Stoichiometric and Catalytic Reactivities of Intermediate B

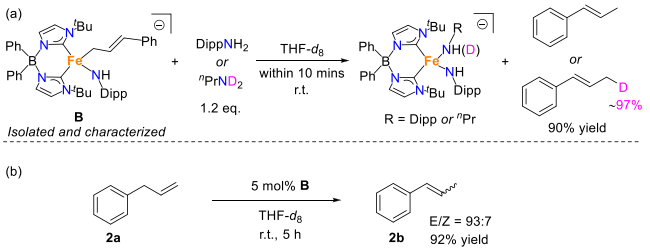

The ^{57}Fe Mössbauer spectral parameters differ from those of the previously reported three-coordinate amido complex Ph$_2$B(^{t}BuIm)$_2$FeN(H)Dipp (δ = 0.47 mm/s and ΔE_Q = 1.39 mm/s).[52] In addition, the three-coordinate amido complex is not observed in the ^{1}H NMR spectrum for the reaction of **1-K(18-C-6)** with **2a** (Figure S61). The spectral data reveal that the reaction of **1-K(18-C-6)** with **2a** does not involve simple proton transfer from allylbenzene to the imido ligand.

Complex **B** immediately reacts with 1.2 equiv of DippNH$_2$ to generate the known bis(anilido) complex[50] [Ph$_2$B(^{t}BuIm)$_2$Fe(NHDipp)$_2$]$^-$ with concomitant formation of prop-1-en-1-ylbenzene **2b** (90% yield). Similarly, reaction with ^{n}PrND$_2$ generates [Ph$_2$B(^{t}BuIm)$_2$Fe(NHDipp)(ND^{n}Pr)]$^-$ and **2b-d$_1$** (Scheme 4a, Figures S62−S65). Importantly, the methyl group in **2b-d$_1$** is deuterated at the same level as observed under catalytic conditions (Scheme 3c). These results strongly support the presence of an η^1-allyl group.

Together, the spectroscopic and reactivity studies suggest that the reaction of **1-K(18-C-6)** with equimolar allylbenzene involves the cooperative action of an iron center and imido ligand to afford the Fe(II) η^1-allyl amido complex [Ph$_2$B(^{t}BuIm)$_2$Fe(NHDipp)(η^1-H$_2$CC(H)═C(H)Ph]$^-$ (**B**). This is also supported by the results of DFT computations (see below). Importantly, **B** is catalytically competent for double bond transposition. The rate of reaction and *E*/*Z* selectivity

https://doi.org/10.1021/jacs.2c13350
J. Am. Chem. Soc. 2023, 145, 11978−11987

(**2a** substrate) are the same as those with **1-K(18-C-6)** catalyst (Scheme 4b). Finally, this species is spectroscopically observed under catalytic conditions using **1-K(18-C-6)**, suggesting that it is the catalyst resting state (Figure S66).

Computational Mechanistic Studies. The combined mechanistic experiments are most consistent with a catalytic cycle in which the iron center and basic imido ligand cooperatively facilitate 1,3-proton transfer in the alkene substrate (Figure 3a). This mechanism is also supported by the results of experimentally calibrated DFT (BP86/B2/SMD//M06L/B1/GP) calculations (Figure 3).

Starting from the Fe(II) imido complex **1-K(18-C-6)**, the alkene **2a** coordinates to the iron center to afford intermediate **A**. Subsequent intramolecular proton transfer from the benzylic proton to the basic imido ligand, followed by double bond transposition, provides the amido η^1-allyl species **B**. It is to be noted that **B** is calculated to be lower 16.3 kcal/mol in energy than its η^3-allyl **B** isomer (Figure S85). In addition, **B** is calculated to be the lowest energy species on the reaction coordinate. It is notable that the structure of **B** is the same as that proposed for the product of the stoichiometric reaction of **1-K(18-C-6)** with allylbenzene **2a** (see above), which is also suggested to be the catalyst resting state.

A second intramolecular proton transfer from **B** leads to release of the double bond transposed alkene **2b**, concomitant with regeneration of the Fe(II) imido complex, thereby closing the catalytic cycle.[67,68] The DFT calculations reveal that the second proton transfer step is rate determining, with an activation barrier (23.4 kcal/mol) that is consistent with the experimentally determined value ($\Delta G^{\ddagger}$ = 20.3 ± 1.6 kcal/mol at 298.15 K, see Figure S80).

The DFT calculations suggest that there are no spin state changes during the catalytic cycle and that the mechanism occurs exclusively on the quintet spin surface (Figure S85). Importantly, the computed transition state structures reveal that the proton is transferred directly from the coordinated alkene to the imido ligand (^{5}**TS$_{A\text{-}B}$**) and back from the amido ligand to the allyl ligand (^{5}**TS$_{B\text{-}1}$**) without the involvement of iron hydrides (Figure 3b). First, the Fe−H distances in these transition states are ca. 1 Å longer than those observed in crystal structures of paramagnetic Fe−H complexes.[69,70] Second, we are able to identify occupied orbitals in the transition state that span C1···H···N1 unit but do not involve the iron atom (Figures S93 and S94). Finally, a putative Fe−H intermediate is calculated to be 38.0 kcal/mol higher in energy than that of **B** (Figure S85). These observations strongly suggest that iron hydrides are not involved in the reaction mechanism. Further support for the proposed proton transfer process comes from the changes of Mulliken atomic charges for C1 and H atoms in **A** and ^{5}**TS$_{A\text{-}B}$**. In the case of the C1 atom, the charge decreases from +0.22 in **A** to −0.08 in ^{5}**TS$_{A\text{-}B}$**, while for the H atom the charge increases from 0.00 in **A** to +0.22 in ^{5}**TS$_{A\text{-}B}$**. These results are consistent with the results of the Hammett study, which suggests that negative charge develops on C1 in the transition state.

It is worth noting that the DFT computations do not support a mechanism in which the imido ligand acts as a simple base without involvement of the iron center. As detailed in the Supporting Information (Figures S96−S98), pathways that do not involve the iron center are higher in energy or lead to species that are catalytic dead ends.

Consequences of the Mechanism: Transposition by pK_a Dictated Proton Transfer. The experimental and computational results support a unique, nonhydridic mechanism, in which the cooperative action of iron and imido ligand facilitate catalytic alkene transposition. Since intramolecular proton transfer steps are a key feature of the mechanism, we anticipate that transposition will be dictated by the pK_a of the substrate allylic proton.

The estimated pK_a for the conjugate acid of **1-K(18-C-6)**, $Ph_2B(^tBuIm)_2Fe(NHDipp)$ is ca. 36 in DMSO,[71] which is larger than that for strong bases such as $^tBuO^-$ and OH^- (the pK_as of ^{t}BuOH and H_2O in DMSO are 32.2 and 31.4, respectively).[72] This suggests that proton transfer and hence double bond transposition will occur for other alkenes having weakly acidic protons. In support of this hypothesis, we observe double bond transposition of 1,4-pentadiene **12a** (pK_a = 35 in DMSO)[73] to the conjugated alkene **12b** in high yield and *E*/*Z* selectivity (Table 2, entry 1). Interestingly, transposition is faster than for the allylbenzene substrates and is complete within 3 h at room temperature in the presence of 2.5 mol % **1-K(18-C-6)**. This is likely due to the smaller steric profile of 1,4-pentadiene, which leads to faster catalysis. Similarly, 1,4-hexadiene **13a** is catalytically transposed to **13b** in high yield and selectivity (entry 2). In addition to 1,4-dienes, *N*-phenyl allylamines **14a** and **15a**, allyl phenyl sulfide **16a**, allyl boronic acid ester **17a**, allyl silanes **18a** and **19a**, allyl phosphine **20a**, and the allyl heterocycles **21a−24a** also

Table 2. Catalytic 1,3-Proton Transfer of Non-benzylic Alkenes Using 1-K(18-C-6)[a]

Entry	Substrate	Time	*E*/*Z*	Product	Yield
1	**12a**	3 h	80:20	**12b**	81%[b]
2	**13a**	3 h	75:25	**13b**	95%[b]
3	**14a**	48 h	30:70[e]	**14b**	85%[c]
4	**15a**	8 h	20:80	**15b**	96%[c]
5	**16a**	2 h	67:33	**16b**	92%
6	**17a**	24 h	86:14	**17b**	81%[c]
7	**18a**	24 h	90:10	**18b**	90%
8	**19a**	48 h	95:5	**19b**	70%[c]
9	**20a**	1 h	5:95	**20b**	89%
10	**21a**	12 h	28:72	**21b**	96%
11	**22a**	24 h	91:9	**22b**	97%
12	**23a**	1 h	80:20	**23b**	50%[d]
13	**24a**	1 h	93:7	**24b**	41%[d]

[a]Reaction conditions: alkene (0.5 mmol) with 5 mol % **1-K(18-C-6)** at room temperature in 0.5 mL of THF-d_8; yields were obtained by ^{1}H NMR analysis of the crude material using mesitylene as internal standard, except for **17a** (84%), **18a** (93%), and **19a** (78%), and the conversions for other substrates are >99%. [b]2.5 mol % **1-K(18-C-6)** was used. [c]10 mol % **1-K(18-C-6)** at 50 °C. [d]Isolated yield. [e](*E*,*Z*)/(*Z*,*Z*) ratio.

https://doi.org/10.1021/jacs.2c13350
J. Am. Chem. Soc. 2023, 145, 11978−11987

undergo transposition, in all cases in high yields and with high E/Z selectivities (entries 3−13). In some cases, particularly with more congested substrates, mild heating is required for reasonable rates of reaction.

To the best of our knowledge, transition metal catalyzed double bond transposition for many of these substrates has never been reported, likely due to the ability of the donor groups to deactivate the metal center. We attribute the successful double bond transposition of substrates containing potentially coordinating groups such as amines, *N*-heterocycles, and phosphines to the high spin nature of the catalyst, which confers greater resistance to typical catalyst poisons due to repulsion between the (partially) occupied Fe 3d orbitals and σ-donor ligands, as we have previously shown.[74] In the case of **14a**, **15a**, **20a**, and **21a**, the *Z* isomer is the dominant product, possibly due to increased steric interactions with these bulkier substrates.[18] It is worth noting that under the same catalytic conditions catalytic transposition of **17a** is not observed using the strong bases ^{t}BuOK and ^{n}PrNHLi. Only stoichiometric conversion is observed with DippNHK. Similarly, ^{t}BuOK provided lower conversions for **18a** (~60%). This suggests that **1-K(18-C-6)** has better tolerance of substrates containing Lewis acid functionality than do these simple bases.

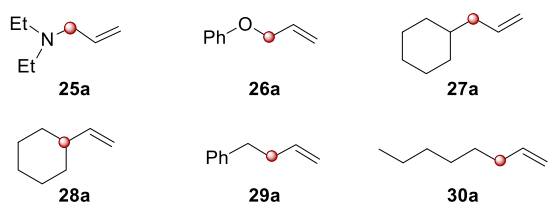

Figure 4. Unreactive, less acidic substrates.

Alkene transposition does not occur for substrates **25a−30a** (Figure 4). No reaction is observed, even after extended heating in the presence of 5 mol % **1-K(18-C-6)**. It is notable that there are no heteroatom-containing functional groups for four of these substrates (**27a−30a**), indicating that the lack of transposition is unlikely due to catalyst poisoning. Indeed, based on the theoretically predicted pK_a values obtained from graph convolutional neural networks,[75] there is an excellent correlation between the propensity to undergo transposition and the acidity of the allylic protons in these substrates (Figure 5). This analysis reveals that the cutoff for transposition occurs at pK_a ≈ 35−36 for the substrate allylic proton.

Based on the observed substrate selectivity, we hypothesized that **1-K(18-C-6)** would selectively transpose alkenes in substrates containing two or more double bonds, as dictated by the pK_a of allylic protons. We tested this hypothesis using a series of substrates that contain groups shown to undergo transposition (i.e., allylbenzene, 1,4-diene, *N*-phenyl allylamine, and allyl phenyl sulfide) as well as 1-alkenes that are inactive toward double bond transposition (**31a−35a**, Table 3).

Table 3. Examples for Regioselective Alkene Transposition Dictated by pK_a of Allylic Protons[a]

Entry	Substrate	Time	*E*/*Z*	Product	Yield
1	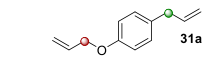 **31a**	48 h	92:8	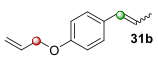 **31b**	81%
2	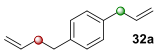 **32a**	24 h	86:14	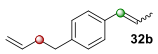 **32b**	70%
3	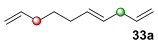 **33a**	5 h	80:20	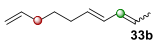 **33b**	83%
4	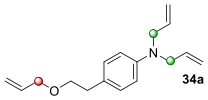 **34a**	4 d	26:74[c]	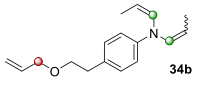 **34b**	86%[b]
5	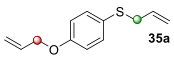 **35a**	12 h	64:36	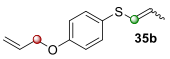 **35b**	88%

[a]Reaction conditions: 1.0 mol/L alkene in THF with 5 mol % **1-K(18-C-6)** at 50 °C; isolated yields reported, and the conversions for the substrates are >99%. [b]10 mol % **1-K(18-C-6)**, NMR yield using mesitylene as the internal standard. [c](*E*,*Z*)/(*Z*,*Z*) ratio.

Gratifyingly, in all cases double bond transposition exclusively occurs at the predicted positions, with the other 1-alkenes in the substrates remaining untouched. The congruence between the predicted and experimental outcomes also provides strong support for the proposed reaction mechanism.

CONCLUSION

In summary, we found that the three-coordinate, high-spin Fe(II) imido complex **1-K(18-C-6)** catalyzes double bond transposition in 1-alkenes to afford the corresponding 2-alkenes. This transition metal catalyst operates by a unique mechanism in which iron and the imido ligand cooperatively facilitate transposition by 1,3-proton transfer from a coordinated 1-alkene substrate, enabling transposition to be dictated by the acidity of the substrate allylic protons. Consequently,

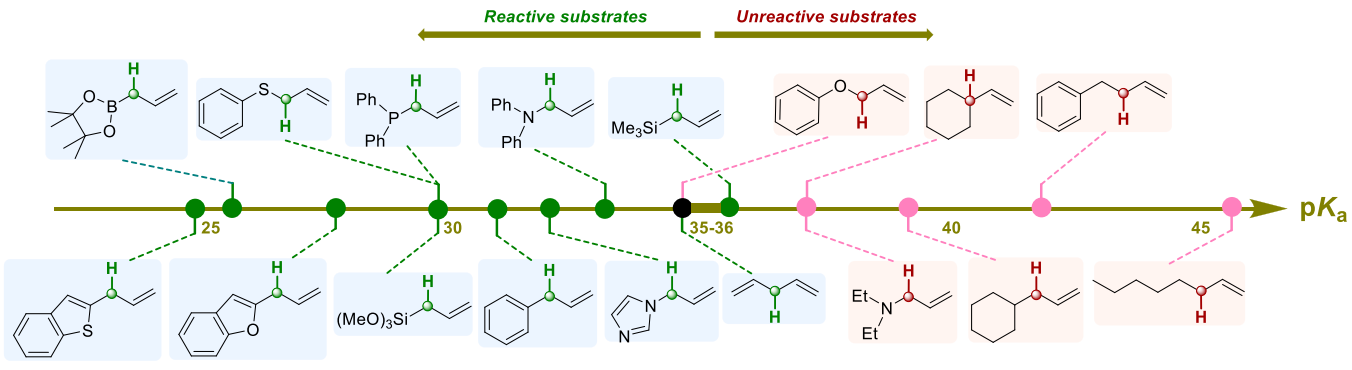

Figure 5. Predicted pK_a trend of the allylic protons in the representative alkenes based on graph convolutional neural networks.

https://doi.org/10.1021/jacs.2c13350
J. Am. Chem. Soc. 2023, 145, 11978−11987

the catalyst facilitates the regioselective transposition of double bonds in substrates containing multiple 1-alkenes. The regioselectivity is predictable, as dictated by the pK_a of the substrate allylic protons. These results also suggest new avenues for metal imido complexes beyond nitrene transfer catalysis, which we are actively investigating.

■ ASSOCIATED CONTENT

Supporting Information

The Supporting Information is available free of charge at https://pubs.acs.org/doi/10.1021/jacs.2c13350.

Full experimental details (PDF)

Cartesian coordinates for the DFT-optimized structures (XYZ)

■ AUTHOR INFORMATION

Corresponding Authors

Hao Tang − *College of Chemistry and Materials Engineering, Wenzhou University, Wenzhou, Zhejiang 325035, P. R. China*; orcid.org/0000-0003-0323-0349; Email: tanghao@wzu.edu.cn

Jeremy M. Smith − *Department of Chemistry, Indiana University, Bloomington, Indiana 47405, United States*; orcid.org/0000-0002-3206-4725; Email: smith962@indiana.edu

Authors

Yafei Gao − *Department of Chemistry, Indiana University, Bloomington, Indiana 47405, United States*; orcid.org/0000-0001-7970-8535

Xuelian Li − *College of Chemistry and Materials Engineering, Wenzhou University, Wenzhou, Zhejiang 325035, P. R. China*

Jeremiah E. Stevens − *Department of Chemistry and Biochemistry, The Ohio State University, Columbus, Ohio 43210, United States*; orcid.org/0000-0002-9419-5835

Complete contact information is available at: https://pubs.acs.org/10.1021/jacs.2c13350

Notes

The authors declare no competing financial interest.

■ ACKNOWLEDGMENTS

This material is based upon work supported by the U.S. Department of Energy, Office of Science, Office of Basic Energy Sciences under Award Number DE-SC0019466. Y.G. and J.M.S. also thank the NSF for financial support (OMA-1936353). H.T. is thankful for the financial support from Zhejiang Provincial Natural Science Foundation of China (Grant No. LQ22B030004) and Wenzhou Municipal Science and Technology Bureau (No. G20220023). We are grateful to Thomas N. Snaddon for helpful comments.

■ REFERENCES

(1) Alcaide, B.; Almendros, P.; Luna, A. Grubbs' Ruthenium-Carbenes Beyond the Metathesis Reaction: Less Conventional Non-Metathetic Utility. *Chem. Rev.* **2009**, *109*, 3817−3858.

(2) Hassam, M.; Taher, A.; Arnott, G. E.; Green, I. R.; van Otterlo, W. A. Isomerization of Allylbenzenes. *Chem. Rev.* **2015**, *115*, 5462−5569.

(3) Larsen, C. R.; Grotjahn, D. B. The Value and Application of Transition Metal Catalyzed Alkene Isomerization in Industry. *Applied Homogeneous Catalysis with Organometallic Compounds*; Wiley-VCH: 2017; pp 1365−1378.

(4) Molloy, J. J.; Morack, T.; Gilmour, R. Positional and Geometrical Isomerisation of Alkenes: The Pinnacle of Atom Economy. *Angew. Chem., Int. Ed.* **2019**, *58*, 13654−13664.

(5) Gauthier, D.; Lindhardt, A. T.; Olsen, E. P. K.; Overgaard, J.; Skrydstrup, T. In Situ Generated Bulky Palladium Hydride Complexes as Catalysts for the Efficient Isomerization of Olefins. Selective Transformation of Terminal Alkenes to 2-Alkenes. *J. Am. Chem. Soc.* **2010**, *132*, 7998−8009.

(6) Larsen, C. R.; Grotjahn, D. B. Stereoselective Alkene Isomerization over One Position. *J. Am. Chem. Soc.* **2012**, *134*, 10357−10360.

(7) Schmidt, A.; Nodling, A. R.; Hilt, G. An Alternative Mechanism for the Cobalt-Catalyzed Isomerization of Terminal Alkenes to (*Z*)-2-Alkenes. *Angew. Chem., Int. Ed.* **2015**, *54*, 801−804.

(8) Kita, M. R.; Miller, A. J. M. An Ion-Responsive Pincer-Crown Ether Catalyst System for Rapid and Switchable Olefin Isomerization. *Angew. Chem., Int. Ed.* **2017**, *56*, 5498−5502.

(9) Wang, Y.; Qin, C.; Jia, X.; Leng, X.; Huang, Z. An Agostic Iridium Pincer Complex as a Highly Efficient and Selective Catalyst for Monoisomerization of 1-Alkenes to trans-2-Alkenes. *Angew. Chem., Int. Ed.* **2017**, *56*, 1614−1618.

(10) Kapat, A.; Sperger, T.; Guven, S.; Schoenebeck, F. Olefins Through Intramolecular Radical Relocation. *Science* **2019**, *363*, 391−396.

(11) Yu, X.; Zhao, H.; Li, P.; Koh, M. J. Iron-Catalyzed Tunable and Site-Selective Olefin Transposition. *J. Am. Chem. Soc.* **2020**, *142*, 18223−18230.

(12) Kawamura, K. E.; Chang, A. S.-m.; Martin, D. J.; Smith, H. M.; Morris, P. T.; Cook, A. K. Modular Ni(0)/Silane Catalytic System for the Isomerization of Alkenes. *Organometallics* **2022**, *41*, 486−496.

(13) Liu, X.; Li, B.; Liu, Q. Base-Metal-Catalyzed Olefin Isomerization Reactions. *Synthesis* **2019**, *51*, 1293−1310.

(14) Liu, X.; Zhang, W.; Wang, Y.; Zhang, Z. X.; Jiao, L.; Liu, Q. Cobalt-Catalyzed Regioselective Olefin Isomerization Under Kinetic Control. *J. Am. Chem. Soc.* **2018**, *140*, 6873−6882.

(15) Liu, X.; Rong, X.; Liu, S.; Lan, Y.; Liu, Q. Cobalt-Catalyzed Desymmetric Isomerization of Exocyclic Olefins. *J. Am. Chem. Soc.* **2021**, *143*, 20633−20639.

(16) Meng, Q. Y.; Schirmer, T. E.; Katou, K.; Konig, B. Controllable Isomerization of Alkenes by Dual Visible-Light-Cobalt Catalysis. *Angew. Chem., Int. Ed.* **2019**, *58*, 5723−5728.

(17) Camp, A. M.; Kita, M. R.; Blackburn, P. T.; Dodge, H. M.; Chen, C. H.; Miller, A. J. M. Selecting Double Bond Positions with a Single Cation-Responsive Iridium Olefin Isomerization Catalyst. *J. Am. Chem. Soc.* **2021**, *143*, 2792−2800.

(18) Chen, C.; Dugan, T. R.; Brennessel, W. W.; Weix, D. J.; Holland, P. L. *Z*-Selective Alkene Isomerization by High-Spin Cobalt(II) Complexes. *J. Am. Chem. Soc.* **2014**, *136*, 945−955.

(19) van Otterlo, W. A.; de Koning, C. B. Metathesis in the Synthesis of Aromatic Compounds. *Chem. Rev.* **2009**, *109*, 3743−3782.

(20) Crossley, S. W.; Barabe, F.; Shenvi, R. A. Simple, Chemoselective, Catalytic Olefin Isomerization. *J. Am. Chem. Soc.* **2014**, *136*, 16788−16791.

(21) Li, G.; Kuo, J. L.; Han, A.; Abuyuan, J. M.; Young, L. C.; Norton, J. R.; Palmer, J. H. Radical Isomerization and Cycloisomerization Initiated by H• Transfer. *J. Am. Chem. Soc.* **2016**, *138*, 7698−7704.

(22) Kim, D.; Pillon, G.; DiPrimio, D. J.; Holland, P. L. Highly *Z*-Selective Double Bond Transposition in Simple Alkenes and Allylarenes through a Spin-Accelerated Allyl Mechanism. *J. Am. Chem. Soc.* **2021**, *143*, 3070−3074.

(23) Biswas, S. Mechanistic Understanding of Transition-Metal-Catalyzed Olefin Isomerization: Metal-Hydride Insertion-Elimination *vs.* π-Allyl Pathways. *Comments Inorg. Chem.* **2015**, *35*, 300−330.

(24) Larionov, E.; Li, H.; Mazet, C. Well-Defined Transition Metal Hydrides in Catalytic Isomerizations. *Chem. Commun.* **2014**, *50*, 9816−9826.
(25) Cram, D. J.; Uyeda, R. T. Electrophilic Substitution at Saturated Carbon. XXII. Intramolecular Hydrogen Transfer Reactions in Base-Catalyzed Allylic Rearrangements. *J. Am. Chem. Soc.* **1964**, *86*, 5466−5477.
(26) Ela, S. W.; Cram, D. J. Electrophilic Substitution at Saturated Carbon. XXX. Behavior of Phenylallylic Anions and Their Conjugate Acids. *J. Am. Chem. Soc.* **1966**, *88*, 5791−5802.
(27) Higashi, T.; Kusumoto, S.; Nozaki, K. Cleavage of Si-H, B-H, and C-H Bonds by Metal-Ligand Cooperation. *Chem. Rev.* **2019**, *119*, 10393−10402.
(28) El-Sepelgy, O.; Brzozowska, A.; Azofra, L. M.; Jang, Y. K.; Cavallo, L.; Rueping, M. Experimental and Computational Study of an Unexpected Iron-Catalyzed Carboetherification by Cooperative Metal and Ligand Substrate Interaction and Proton Shuttling. *Angew. Chem., Int. Ed.* **2017**, *56*, 14863−14867.
(29) Galiana-Cameo, M.; Urriolabeitia, A.; Barrenas, E.; Passarelli, V.; Pérez-Torrente, J. J.; Di Giuseppe, A.; Polo, V.; Castarlenas, R. Metal−Ligand Cooperative Proton Transfer as an Efficient Trigger for Rhodium-NHC-Pyridonato Catalyzed gem-Specific Alkyne Dimerization. *ACS Catal.* **2021**, *11*, 7553−7567.
(30) Virant, M.; Mihelac, M.; Gazvoda, M.; Cotman, A. E.; Frantar, A.; Pinter, B.; Kosmrlj, J. Pyridine Wingtip in $[Pd(Py\text{-}tzNHC)_2]^{2+}$ Complex Is a Proton Shuttle in the Catalytic Hydroamination of Alkynes. *Org. Lett.* **2020**, *22*, 2157−2161.
(31) Grotjahn, D. B.; Larsen, C. R.; Gustafson, J. L.; Nair, R.; Sharma, A. Extensive Isomerization of Alkenes Using a Bifunctional Catalyst: An Alkene Zipper. *J. Am. Chem. Soc.* **2007**, *129*, 9592−9593.
(32) Erdogan, G.; Grotjahn, D. B. Mild and Selective Deuteration and Isomerization of Alkenes by a Bifunctional Catalyst and Deuterium Oxide. *J. Am. Chem. Soc.* **2009**, *131*, 10354−10355.
(33) Cao, T. C.; Cooksy, A. L.; Grotjahn, D. B. Origins of High Kinetic (*E*)-Selectivity in Alkene Isomerization by a CpRu(PN) Catalyst: a Combined Experimental and Computational Approach. *ACS Catal.* **2020**, *10*, 15250−15258.
(34) King, E. R.; Hennessy, E. T.; Betley, T. A. Catalytic C-H Bond Amination From High-Spin Iron Imido Complexes. *J. Am. Chem. Soc.* **2011**, *133*, 4917−4923.
(35) Zhang, L.; Deng, L. C-H Bond Amination by Iron-Imido/Nitrene Species. *Chin. Sci. Bull.* **2012**, *57*, 2352−2360.
(36) Hennessy, E. T.; Betley, T. A. Complex N-Heterocycle Synthesis via Iron-Catalyzed, Direct C−H Bond Amination. *Science* **2013**, *340*, 591−595.
(37) Hennessy, E. T.; Liu, R. Y.; Iovan, D. A.; Duncan, R. A.; Betley, T. A. Iron-Mediated Intermolecular N-Group Transfer Chemistry with Olefinic Substrates. *Chem. Sci.* **2014**, *5*, 1526−1532.
(38) Du, J.; Wang, L.; Xie, M.; Deng, L. A Two-Coordinate Cobalt(II) Imido Complex with NHC Ligation: Synthesis, Structure, and Reactivity. *Angew. Chem., Int. Ed.* **2015**, *54*, 12640−12644.
(39) Wang, L.; Hu, L.; Zhang, H.; Chen, H.; Deng, L. Three-Coordinate Iron(IV) Bisimido Complexes with Aminocarbene Ligation: Synthesis, Structure, and Reactivity. *J. Am. Chem. Soc.* **2015**, *137*, 14196−14207.
(40) Iovan, D. A.; Betley, T. A. Characterization of Iron-Imido Species Relevant for N-Group Transfer Chemistry. *J. Am. Chem. Soc.* **2016**, *138*, 1983−1993.
(41) Wilding, M. J. T.; Iovan, D. A.; Betley, T. A. High-Spin Iron Imido Complexes Competent for C-H Bond Amination. *J. Am. Chem. Soc.* **2017**, *139*, 12043−12049.
(42) Wilding, M. J. T.; Iovan, D. A.; Wrobel, A. T.; Lukens, J. T.; MacMillan, S. N.; Lancaster, K. M.; Betley, T. A. Direct Comparison of C-H Bond Amination Efficacy through Manipulation of Nitrogen-Valence Centered Redox: Imido versus Iminyl. *J. Am. Chem. Soc.* **2017**, *139*, 14757−14766.
(43) Bagchi, V.; Kalra, A.; Das, P.; Paraskevopoulou, P.; Gorla, S.; Ai, L.; Wang, Q.; Mohapatra, S.; Choudhury, A.; Sun, Z.; Cundari, T. R.; Stavropoulos, P. Comparative Nitrene-Transfer Chemistry to Olefinic Substrates Mediated by a Library of Anionic Mn(II) Triphenylamido-Amine Reagents and M(II) Congeners (M = Fe, Co, Ni) Favoring Aromatic over Aliphatic Alkenes. *ACS Catal.* **2018**, *8*, 9183−9206.
(44) Wang, P.; Deng, L. Recent Advances in Iron-Catalyzed C-H Bond Amination via Iron Imido Intermediate. *Chin. J. Chem.* **2018**, *36*, 1222−1240.
(45) Cheng, J.; Liu, J.; Leng, X.; Lohmiller, T.; Schnegg, A.; Bill, E.; Ye, S.; Deng, L. A Two-Coordinate Iron(II) Imido Complex with NHC Ligation: Synthesis, Characterization, and Its Diversified Reactivity of Nitrene Transfer and C-H Bond Activation. *Inorg. Chem.* **2019**, *58*, 7634−7644.
(46) Cao, C.; Mao, G.; Cheng, J.; Leng, X.; Deng, L. Reactions of a Bis(vinyltrimethylsilane)nickel(0) N-Heterocyclic Carbene Complex with Organic Azides. *J. Organomet. Chem.* **2020**, *913*, 121195−121203.
(47) Kawakita, K.; Kakiuchi, Y.; Tsurugi, H.; Mashima, K.; Parker, B. F.; Arnold, J.; Tonks, I. A. Reactivity of Terminal Imido Complexes of Group 4−6 Metals: Stoichiometric and Catalytic Reactions Involving Cycloaddition with Unsaturated Organic Molecules. *Coord. Chem. Rev.* **2020**, *407*, 213118.
(48) Liu, Q.; Long, L.; Ma, P.; Ma, Y.; Leng, X.; Xiao, J.; Chen, H.; Deng, L. Synthesis, Structure, and C−H Bond Activation Reaction of an Iron(IV) Terminal Imido Complex Bearing Trifluoromethyl Groups. *Cell Rep. Phys. Sci.* **2021**, *2*, 100454.
(49) La Pierre, H. S.; Arnold, J.; Toste, F. D. *Z*-Selective Semihydrogenation of Alkynes Catalyzed by a Cationic Vanadium Bisimido Complex. *Angew. Chem., Int. Ed.* **2011**, *50*, 3900−3903.
(50) Gao, Y.; Carta, V.; Pink, M.; Smith, J. M. Catalytic Carbodiimide Guanylation by a Nucleophilic, High Spin Iron(II) Imido Complex. *J. Am. Chem. Soc.* **2021**, *143*, 5324−5329.
(51) Gao, Y.; Pink, M.; Carta, V.; Smith, J. M. Ene Reactivity of an Fe═NR Bond Enables the Catalytic α-Deuteration of Nitriles and Alkynes. *J. Am. Chem. Soc.* **2022**, *144*, 17165−17172.
(52) Gao, Y.; Pink, M.; Smith, J. M. Alkali Metal Ions Dictate the Structure and Reactivity of an Iron(II) Imido Complex. *J. Am. Chem. Soc.* **2022**, *144*, 1786−1794.
(53) Bordwell, F. G.; Van der Puy, M.; Vanier, N. R. Carbon Acids. 9. The Effects of Divalent Sulfur and Divalent Oxygen on Carbanion Stabilities. *J. Org. Chem.* **1976**, *41*, 1885−1886.
(54) Bowden, K.; Cook, S. R. Reactions in Strongly Basic Solutions. Part VI. Correlation of the Rates of Rearrangement of Weak Carbon Acids in Aqueous Dimethyl Sulfoxide with an Acidity Function. Substituent and Kinetic Isotope Effects. *J. Chem. Soc., Perkin Trans.* **1972**, *2*, 1407−1411.
(55) Scarso, A.; Colladon, M.; Sgarbossa, P.; Santo, C.; Michelin, R. A.; Strukul, G. Highly Active and Selective Platinum(II)-Catalyzed Isomerization of Allylbenzenes: Efficient Access to (*E*)-Anethole and Other Fragrances via Unusual Agostic Intermediates. *Organometallics* **2010**, *29*, 1487−1497.
(56) Garhwal, S.; Kaushansky, A.; Fridman, N.; de Ruiter, G. Part per Million Levels of an Anionic Iron Hydride Complex Catalyzes Selective Alkene Isomerization via Two-State Reactivity. *Chem. Catal.* **2021**, *1*, 631−647.
(57) Woof, C. R.; Durand, D. J.; Fey, N.; Richards, E.; Webster, R. L. Iron Catalyzed Double Bond Isomerization: Evidence for an Fe^{I}/Fe^{III} Catalytic Cycle. *Chem.—Eur. J.* **2021**, *27*, 5972−5977.
(58) Che, C. M.; Zhou, C. Y.; Wong, L. M. Catalysis by Fe═X Complexes (X = NR, CR_2). *Top. Organomet. Chem.* **2011**, *33*, 111−138.
(59) Gianetti, T. L.; La Pierre, H. S.; Arnold, J. Group 5 Imides and Bis(imide)s as Selective Hydrogenation Catalysts. *Eur. J. Inorg. Chem.* **2013**, *2013*, 3771−3783.
(60) While we have never observed free $DippNH^-$ in any chemistry involving **1-K(18-C-6)** (see for example refs 50−52), it is possible that the imido complex serves as a source of this base.
(61) This result also suggests that a mechanism in which alkene coordination activates **1-K(18-C-6)** towards outer sphere proton transfer from an additional molecule of substrate is unlikely. In such a

mechanism, the bulkier and electron-withdrawing *cis*-stilbene ligand would be expected to dramatically attenuate the rate of reaction by hindering access to the imido ligand as well as decreasing its basicity. However, the rate of catalysis in the presence of *cis*-stilbene (k_{obs} = 5.67 × 10^{-5} s^{-1}) is actually slightly faster than that observed in the presence of 1-octene (k_{obs} = 2.83 × 10^{-5} s^{-1}).

(62) Bank, S.; Schriesheim, A.; Rowe, C. A., Jr. An Understanding of the Stereoselectivity of Base-Catalyzed Olefin Isomerization Based on a Thermodynamically More Stable *cis*-Allylic Anion. *J. Am. Chem. Soc.* **1965**, *87*, 3244−3245.

(63) Since the reaction is slow at room temperature, moderate heating is required to drive it at reasonable rates.

(64) Whether the origin of this large KIE is due to tunneling or other factors is not clear at this stage. We tentatively suggest that it is the consequence of multiple steps involving proton transfer. More detailed investigations into the origin of the large KIE are in progress.

(65) The rate of transposition of **2a-d$_2$** is too slow to be measured at room temperature, while at 45 °C, the rate is too fast to be measued for **2a**. Consequently, the KIE was determined at 40 °C.

(66) Although the formation of free ^{n}PrNH^{-} is also unlikely (ref 60), it is possible that it could be formed by the deprotonation of ^{n}PrNH$_2$ by the basic imido ligand in **1-K(18-C-6)**.

(67) Bennett, J. L.; Wolczanski, P. T. Energetics of C-H Bond Activation and Ethylene Binding to d0 Transient (silox)$_2$Ti═NSi^{t}Bu$_3$. *J. Am. Chem. Soc.* **1994**, *116*, 2179−2180.

(68) Polse, J. L.; Andersen, R. A.; Bergman, R. G. Reactivity of a Terminal Ti(IV) Imido Complex toward Alkenes and Alkynes: Cycloaddition *vs* C-H Activation. *J. Am. Chem. Soc.* **1998**, *120*, 13405−13414.

(69) Gu, N. X.; Oyala, P. H.; Peters, J. C. An S = 1/2 Iron Complex Featuring N_2, Thiolate, and Hydride Ligands: Reductive Elimination of H_2 and Relevant Thermochemical Fe-H Parameters. *J. Am. Chem. Soc.* **2018**, *140*, 6374−6382.

(70) Chiang, K. P.; Scarborough, C. C.; Horitani, M.; Lees, N. S.; Ding, K.; Dugan, T. R.; Brennessel, W. W.; Bill, E.; Hoffman, B. M.; Holland, P. L. Characterization of the Fe-H Bond in a Three-Coordinate Terminal Hydride Complex of Iron(I). *Angew. Chem., Int. Ed.* **2012**, *51*, 3658−3662.

(71) The pK_a of Ph$_2$B(^{t}BuIm)$_2$Fe(NHDipp) was estimated to be 42.2 in THF (see ref 51), and the conversion in DMSO was according to: Tshepelevitsh, S.; Kütt, A.; Lõkov, M.; Kaljurand, I.; Saame, J.; Heering, A.; Plieger, P. G.; Vianello, R.; Leito, I. On the Basicity of Organic Bases in Different Media. *Eur. J. Org. Chem.* **2019**, *2019*, 6735−6748.

(72) Olmstead, W. N.; Margolin, Z.; Bordwell, F. G. Acidities of Water and Simple Alcohols in Dimethyl Sulfoxide Solution. *J. Org. Chem.* **1980**, *45*, 3295−3299.

(73) Bordwell, F. G.; Drucker, G. E.; Fried, H. E. Acidities of Carbon and Nitrogen Acids: the Aromaticity of the Cyclopentadienyl Anion. *J. Org. Chem.* **1981**, *46*, 632−635.

(74) Lutz, S. A.; Hickey, A. K.; Gao, Y.; Chen, C. H.; Smith, J. M. Two-State Reactivity in Iron-Catalyzed Alkene Isomerization Confers σ-Base Resistance. *J. Am. Chem. Soc.* **2020**, *142*, 15527−15535.

(75) Roszak, R.; Beker, W.; Molga, K.; Grzybowski, B. A. Rapid and Accurate Prediction of pK_a Values of C-H Acids Using Graph Convolutional Neural Networks. *J. Am. Chem. Soc.* **2019**, *141*, 17142−17149.

https://doi.org/10.1021/jacs.2c13350
J. Am. Chem. Soc. 2023, 145, 11978−11987